ELSEVIER

Finite Elements in Analysis and Design 38 (2002) 613–630

FINITE ELEMENTS IN ANALYSIS AND DESIGN

www.elsevier.com/locate/finel

Nonlinear thermoviscoelastic analysis of solid propellant grains subjected to temperature loading

Shiang-Woei Chyuan[a,b,*]

[a] *Department of Mechanical Engineering, National Taiwan University, Taipei, Taiwan, ROC*
[b] *Chung Shan Institute of Science and Technology, P.O. Box 90008-15-3, Lung-Tan, Tao-Yuan 325, Taiwan, ROC*

Abstract

Traditionally, the nonlinear thermoviscoelastic analysis of solid propellant grains subjected temperature loading was not considered, and quasi-elastic analysis was widely adopted for structural integrity because of simplifying the analytical task. But it does not mean that the nonlinear effect is not useful and could be neglected arbitrarily, and this effect usually plays a very important role for some critical design. In order to simulate the material and geometrical nonlinearities, a step-by-step finite element model accompanied by concepts of time–temperature shift principle, reduced integration and thermorheologically simple material assumption was used. Results show that the material nonlinear effect is important for structural integrity of solid propellant grains under higher temperature surrounding, the effect of nonlinearity is not obvious under lower temperature surrounding, and the differences between linear and nonlinear analysis results become more and more predominant as temperature increases. In addition, the maximum shear stress obtained from the nonlinear simulation considering bulk modulus variation with compressive stresses are higher than those from linear simulation, and the effect of material nonlinearity is more predominant as compared to the effect of geometrical nonlinearity. From the work of linear and nonlinear analyses, the nonlinear thermoviscoelastic analysis highlighted several areas of interest and a more accurate and reasonable result could be obtained for engineer.

Keywords: FEA; Shift factor; Reduced time; Strain rate; Bulk modulus; Geometrical nonlinearity; Material nonlinearity

1. Introduction

Recent developments in numerical techniques and computer simulation methods have resulted in a very prestigious progress in engineering analysis. With the increasing developments of digital

* Corresponding author. Chung Shan Institute of Science and Technology, P.O. Box 90008-15-3, Lung-Tan, Tao-Yuan 325, Taiwan, ROC. Fax: +886-347-13318.
E-mail address: yeaing@iris.seed.net.tw (S.-W. Chyuan).

0168-874X/02/$ - see front matter
PII: S0168-874X(01)00095-6

computer power, finite element method [1,2] was considered to be one of the most powerful CAE design tools for engineers. Complex structural configurations can be modeled using finite elements and the response at any desired point of the structure can easily be determined. In the last, the finite element method has been evolving to be a widely accepted tool for the solution of pragmatic engineering problems.

Solid rocket motor structural design currently is based on the concept of a mechanically weak solid propellant grain cast into a stronger metallic or composite case. The outer case provides the essential structural resistance against service and operational loads, and the inner propellant grain's low strength is used for transmission of loads from the grain surface to the outer case. In general, solid rocket motors are subjected to diverse loading during shipment, storage and firing. It is well known that under these loading conditions, cracks can develop in solid propellants because of excessive loads. Therefore, in order to determine the integrity and the ultimate service life of solid rocket motors, studies should be conducted to evaluate the significance of the value and distribution of stress and strain. In a missile system, the structural configuration of solid rocket motor is one of the most complicated parts, and, numerical techniques are necessary to simulate the physical behavior and to evaluate the structural integrity of the different designs, and, to minimize the cost of product development. During the last two decades, more and more attention has been paid to the design, manufacturing, and evaluation of solid propellant grains in order to meet service life and performance requirements [3]. Meanwhile, it is also recognized that aging studies (for example: mechanical aging [4,5], chemical aging [6,7], etc.) are extremely necessary to predict the service life of solid propellant grains and the thermal response under thermal shock loads [8,9] plays an important role. Therefore, the reduction of thermal response is one of the significant considerations in the primary design of solid propellant grains and some effective designs (for example: free flap design, P-groove design, stress reliever design, etc.) have been adopted [10]. For the time–temperature-dependent behavior of linear viscoelastic and incompressible polymer materials, concept of time–temperature shift principle, reduced integration and thermorheologically simple material (TSM) assumption were widely used in the linear viscoelastic analysis [11–13]. In addition, the method of nonlinear viscoelastic analysis of solid propellant grains for ignition pressurization load was developed [14]. From the above statements concerning solid propellant grains, one can see that it is a very difficult and laborious task to predict the physical response during the design phase. Therefore, the use of computer simulation technique to analyze the structural behavior of solid rocket motor in the preliminary design stage is very important and necessary. Because the nonlinear thermoviscoelastic analysis of solid propellant grains subjected to temperature loading was not considered in the previous papers [3–14], the material and geometrical nonlinearities effects induced by nonlinear bulk modulus cannot be simulated and modeled accurately. But it does not mean that the nonlinear effect is not important and could be negligible arbitrarily, and this effect usually plays a very important role for some critical design. In order to study the effect of geometrical and material nonlinearities, application of nonlinear thermoviscoelastic analysis and five different thermal loading cases were used in the present paper. In this paper, a successful and feasible numerical model following step-by-step thermal loading case was used and discussed thoroughly. Results show that such material nonlinear effect is important for structural integrity of solid propellant grains under higher temperature surrounding, and this effect is not obvious under lower temperature surrounding. In addition, the maximum shear stress obtained from the nonlinear simulation considering bulk modulus variation with compressive stresses are higher than those from linear simulation. From the work of linear and nonlinear analyses, the nonlinear thermoviscoelastic

analysis highlighted several areas of interest and a more accurate and reasonable result could be obtained for engineer. Recommendation resulting from this work has been forwarded to designer successfully, for incorporation of modifications, and to other proper areas for design evaluation.

In engineering analysis, theoretical model was the first choice for researchers and scientists because of totally correct and unique solution. But in the pragmatic design problem, theoretical model was scarcely utilized to predict physical response because of the very complex geometrical design and loading transfer path. In addition, an analytical solution to a viscoelastic problem has only been possible for certain simple configurations and for material properties which are represented by relatively simple viscoelastic models. For the more complex solid rocket motors, numerical or approximate methods have to be used. Therefore, powerful numerical method was introduced to analyst to face the difficulty. Among different numerical approaches, finite element method (FEM) and boundary element method (BEM); and, the increasing developments of digital computer power have moved from being research tools for select groups to become powerful design tools for engineers. For BEM [15], the easy data preparation due to one-dimensional reduction makes it attractive for special practical use. For problems with singularities (for example: seepage flow problems, crack, etc.), it is well known that BEM accompanying with dual integral formulation [16] became a very effective analytical model. However, the main drawback of BEM is that it is not easy to apply in the field of complicated design. In the structural analysis of complex geometrical solid propellant grains, BEM is difficult to apply. Therefore, FEM has become the most widely used numerical technique for analysis of missile system because the extremely complex structural configurations (for example: cylinder head structure [17]) can be modeled using finite elements and the response at any desired point of the structure can easily be determined [18].

2. Finite element modeling

2.1. Fundamentals of finite elements

Basically, nonlinear problems are classified into three broad categories: geometric nonlinearity, material nonlinearity, and contact. For solid rocket motor subjected to diverse thermal loading cases, contact problem could be neglected. Geometrically nonlinear problems involve large displacements; "large" means that the displacements invalidate the small displacement assumptions inherent in the equations of linear analysis. Another aspect of geometrical nonlinear analysis involves follower forces, and capturing this behavior requires the iterative update techniques of nonlinear analysis. In addition, material nonlinear analysis can be used to analyze problems where the stress–strain relationship of the material is nonlinear. For solid propellant grains, the nonlinear effect of bulk modulus variation with compressive stresses is the main goal to be analyzed and investigated.

From an analytical viewpoint, the formulation of a linear elastic static structural problem for a solution by the displacement method is appropriately described by the matrix form

$$[K]\{D\} = \{F\}, \tag{1}$$

where the stiffness matrix $[K]$ is given by

$$[K] = \int\int\int_v [B]^{\mathrm{T}}[D][B]\,\mathrm{d}V, \tag{2}$$

where the matrix [D] is elasticity matrix, and [B] is a matrix relating strains and nodal displacements. But for solid propellant grains under compressive stress distribution, the effect of bulk modulus variation with compressive stress should be considered, and nonlinear analysis following a step-by-step procedure needed to be used. To take into account the geometrical and material nonlinearities in the finite element analysis, an incremental approach is often used for numerical simulation. Therefore, the matrix [D] in Eq. (2) is now variable and is updated at each load step to consider the nonlinear material properties. The geometrical nonlinearity is taken into account by computing stiffness matrix for the deformed configuration, at each load step. The effect of geometrical nonlinearity is incorporated into Eq. (2) by modifying the [B] matrix at each load step, taking into account the change in grain geometry.

2.2. Constitutive model and material properties of solid propellant grains

All modern solid propellant grains utilize an elastomeric binder, which is filled with a quite high level of solid particles. The application of a load cause different mechanisms to take place in the binder, the filler or the interface between them such as the breakage of polymer chains, breakage and reformation of weak bonds, deformation and geometrical rearrangement of filler particles, interfacial debonding, also called dewetting, the formation of microvoids at or near the interface of the particles and surrounding matrix. Under these influences solid propellant grains exhibit very complex behavior including features associated with time and rate effects, temperature and superimposed pressure dependence, large deformations and large strains, stress softening during cyclic loading, and transition from incompressible to compressible behavior. Therefore, the attempt to represent all aspects of solid propellant grain behavior would result in a very complicated constitutive model and would require a wide range of tests to characterize the propellant grains. Thus, a number of previous investigations have been concerned with certain features only. In the present paper, a proper constitutive model [19,20] of solid propellant grains for engineering analysis was used.

$$\sigma(t) = \int_0^t E(t-\tau)[\partial\varepsilon(t)/\partial\tau]\,\mathrm{d}\tau, \tag{3}$$

where $\sigma(t)$ is stress relaxation function, and $E(t)$ is relaxation modulus. The dependence of the viscoelastic properties on the temperature is introduced in a form of an assumption that the solid propellant grain is a rheologically simple material. This assumption permits an introduction of the reduced time ξ which is defined as follows [21]:

$$\xi = \int_0^t \mathrm{d}\tau'/a_T, \tag{4}$$

where a_T is the time–temperature shift function. The consequence of the existence of the reduced time is that a viscoelastic property at some arbitrary temperature T can now be related to the same function at a reference temperature T_0; e.g.,

$$E(T,t) = E(T_0,\xi). \tag{5}$$

The effective propellant modulus, E_{eq}, to be used in the stress and strain analysis, shall be obtained from the master relaxation modulus curve at a temperature-reduced time corresponding to the time required to reach equilibrium, t^*, divided by the shift factor, a_T, for the surrounding temperature;

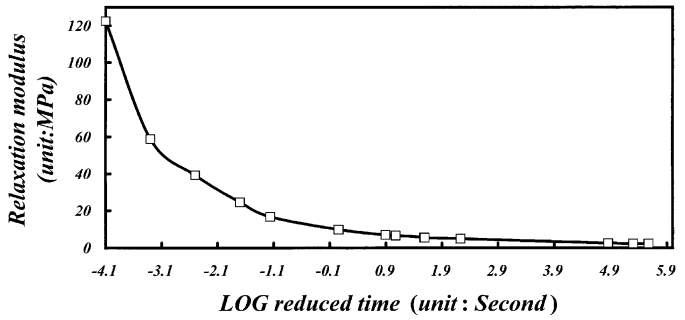

Fig. 1. The master curve of the relaxation modulus for the HTPB propellant.

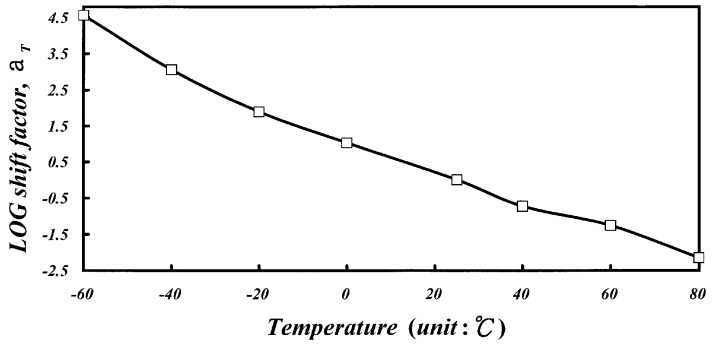

Fig. 2. The time-shift factor for the HTPB propellant.

that is,

$$E_{\mathrm{eq}} = E(t^*/a_T). \tag{6}$$

For the hydroxy terminated polybutadiene binder (HTPB) propellant used in this analysis, the relaxation modulus versus the temperature-reduced time is shown by Fig. 1, and the time-shift factor for the HTPB propellant is shown by Fig. 2. The curves in Figs. 1 and 2 are plotted according to the experimental data in the environment under different temperatures. Propellant failure properties shall be used on master curves of maximum nominal stress, $\sigma_{\max}$, and strain at maximum nominal stress, $\varepsilon_{\max}$, versus temperature-reduced time, t/a_T. The tests used to generate these master curves shall be conducted in accordance with the JANNAF Tentative Standard Uniaxial Test Procedure and at the same temperatures for which relaxation modulus tests were conducted in [22]. The time–temperature shift factors, a_T, obtained from the relaxation modulus tests shall be utilized in constructing the master uniaxial failure curves. The failure criterion for the solid propellant grains depends on its allowable stress and allowable strain, and the strength of the HTPB propellant used in the present paper is obtained from the master allowable stress and allowable strain curve in Figs. 3 and 4. In addition, Poisson's ratio (v_p) and coefficient of linear thermal expansion (α_p) for HTPB propellant from [22] were used in the stress and strain analysis, and Poisson's ratio (v_i) and coefficient of linear thermal expansion (α_i) for liner between outer steel case and inner propellant grains from [22] were

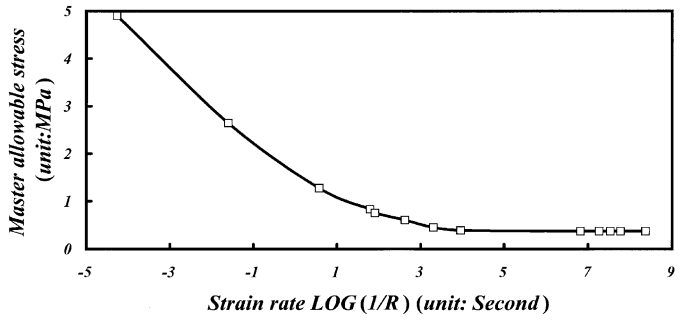

Fig. 3. The master curve of the allowable stress for the HTPB propellant.

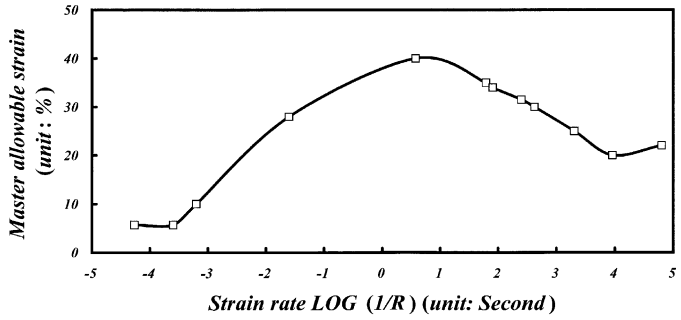

Fig. 4. The master curve of the allowable strain for the HTPB propellant.

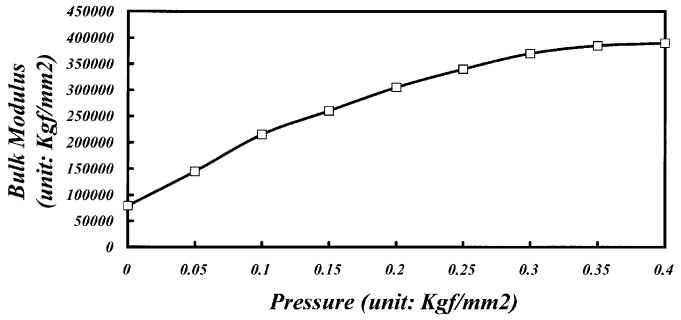

Fig. 5. Variation of bulk modulus with pressure for HTPB-based propellant.

adopted. The reference temperature, T_{SF}, for strain-free and stress-free condition, shall be taken to be 20°F above the propellant cure temperature, T_{cure}, for solid rocket motors which are not pressure cured. In the last, the Young's modulus (E_c), Poisson's ratio (v_c) and thermal expansion coefficient (α_c) for outer steel case from [22] were used in this work. In addition, the data used for the bulk modulus variation with compressive stresses could be found from test or [14] (see Fig. 5).

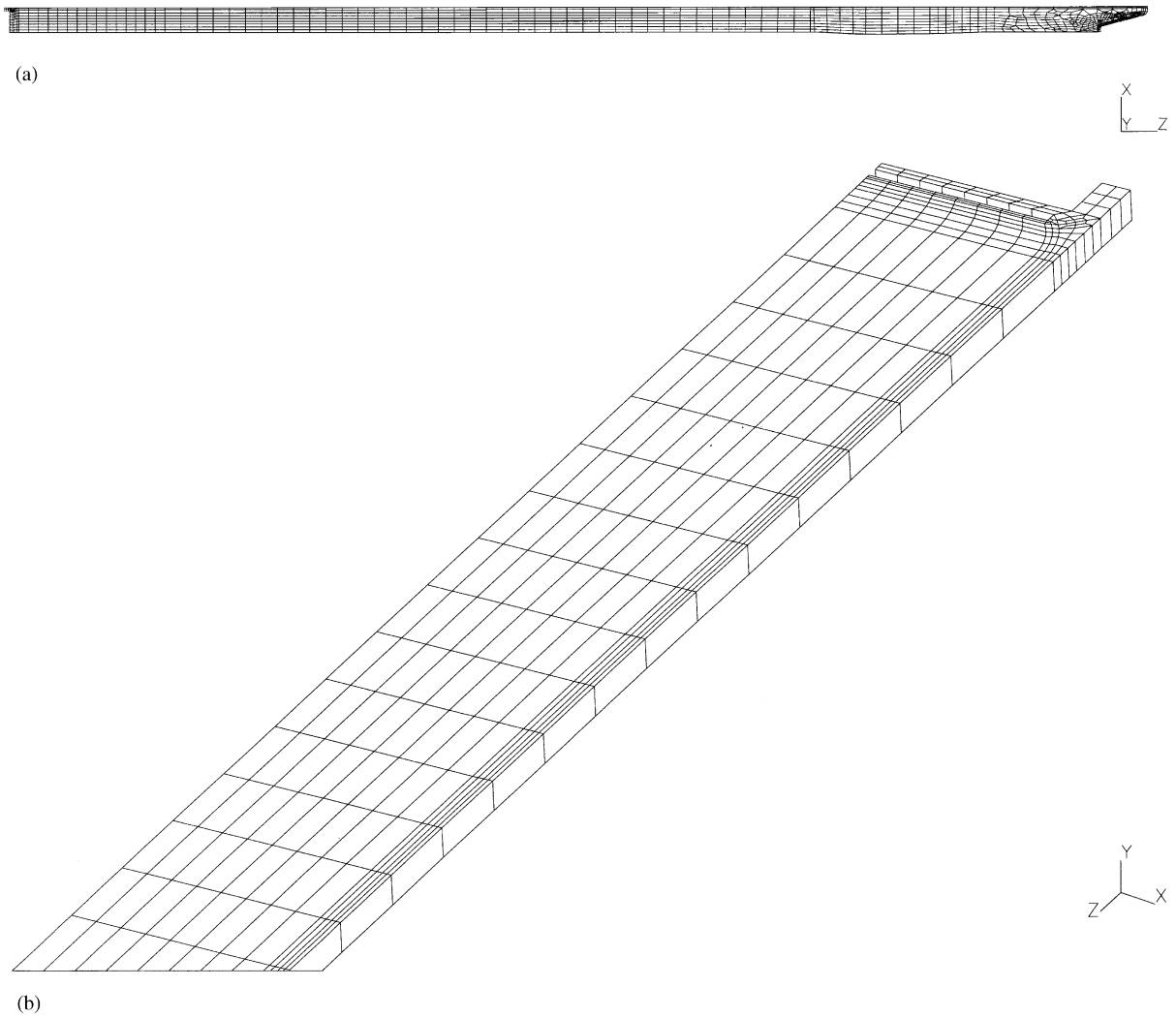

Fig. 6. The finite element model of solid rocket motor.

2.3. Finite element modeling of solid rocket motor and reduced integration

Because of the complexity of geometrical design and load path of solid rocket motor system, it is not easy to model the complicated stiffness distribution of this structure just using a simply analytical model. Therefore, a 3-D solid model was chosen for this structure in order to predict the stress and strain response in detail. The mesh density on some critical areas is much higher than other sub-critical parts in order to reduce the number of degrees of freedom. Due to the symmetry of the geometry and loading, a model of a five-degree segment with axis-symmetric boundary conditions on the cut faces was utilized for simplicity without loss of accuracy. Some appropriate finite element mesh (Fig. 6) with 1408 eight-node solid elements (CHEXA) and 2956

grid nodes were built for the stress and strain analysis, respectively, to acquire their corresponding convergent results. As Poisson's ratio v approaches to 0.5, a material becomes incompressible. For convenience, it is tempting to approximate incompressibility by using $v = 0.49$. But, near $v = 0.5$, stresses are strongly dependent on v — stresses may double as v goes from 0.48 to 0.50. Also, structural equations become ill-conditioned as v approaches to 0.5 and numerical trouble becomes more likely, and finally the mesh "locks". In the present paper, reduced integration [1] was adopted to simulate the nearly incompressible property of the solid propellant grains. In addition, the finite element simulation was executed on an IBM590/RS6000 computer system, the CPU time for a static run under linear viscoelastic analysis case was 57.95 s, and the CPU time for a static run under nonlinear thermoviscoelastic analysis case was 457.4 s.

2.4. Structural integrity of solid propellant grains

Critical regions for stress and strain throughout the solid propellant grain and propellant/liner/insulation bond system shall be identified. The strain and stress failure criterion described below shall be applied to all critical surface-strain locations. The failure criteria are expressed in terms of the propellant grain, including surface locations and the propellant/liner/insulation bond system.

3. Thermal loading case of solid rocket motor system

For missile system, the reference temperature, T_{SF}, for motors which are pressure cured shall be taken to be the highest required storage temperature (the propellant cure temperature is T_{cure}), and the solid rocket motor will be placed at the surrounding of storage temperature $T_{storage}$ (for example: $+77^{\circ}$F) during the period time of $t_{cooldowm}$ (for example: 5 days) for thermal cooldown to equilibrium. After thermal equilibrium, the motor will be taken to place at the surrounding of the operating temperature $T_{operating}$, then the motor will be used in the static test. In addition, five diverse thermal loading case assumptions were chosen, analyzed and discussed.

Thermal loading case 1:

$$T_{SF} = +160\circ\text{F}, \quad T_{operating} = +77\circ\text{F}; \quad t_{cooldown} = 5 \text{ days}.$$

Thermal loading case 2:

$$T_{SF} = +160\circ\text{F}, \quad T_{operating} = +142\circ\text{F}; \quad t_{cooldown} = 5 \text{ days}.$$

Thermal loading case 3:

$$T_{SF} = +160\circ\text{F}, \quad T_{operating} = +169\circ\text{F}; \quad t_{cooldown} = 5 \text{ days}.$$

Thermal loading case 4:

$$T_{SF} = +160\circ\text{F}, \quad T_{operating} = +178\circ\text{F}; \quad t_{cooldown} = 5 \text{ days}.$$

Thermal loading case 5:

$$T_{SF} = +160^{\circ}F, \quad T_{operating} = +205^{\circ}F; \quad t_{cooldown} = 5 \text{ days}.$$

4. Finite element analysis

4.1. Thermal loading case 1 ($T_{SF} = +160^{\circ}F, T_{operating} = +77^{\circ}F; t_{cooldown} = 5$days)

4.1.1. Quasi-elastic linear analysis

Under this thermal loading condition, the design load is defined as $T_{design} = (T_{operating} - T_{SF}) = -83^{\circ}F$ and the effective propellant modulus ($E_{eq} = E(t^*/a_T)$) could be obtained from Fig. 1, and the shift factor ($\log a_T$) could be obtained from Fig. 2. From the linear finite element simulation without the effect of geometrical and material nonlinearities to HTPB propellant, the maximum displacement δ_{max,Δ_T} is 1.03 mm, the maximum principal stress σ_{max,Δ_T} is 0.0187 kgf/mm^2 (see Fig. 7), the maximum shear stress τ_{max,Δ_T} is 0.00843 kgf/mm^2 (see Fig. 8), and the maximum principal strain $\varepsilon_{max,\Delta_T}$ is 4.98% (see Fig. 9).

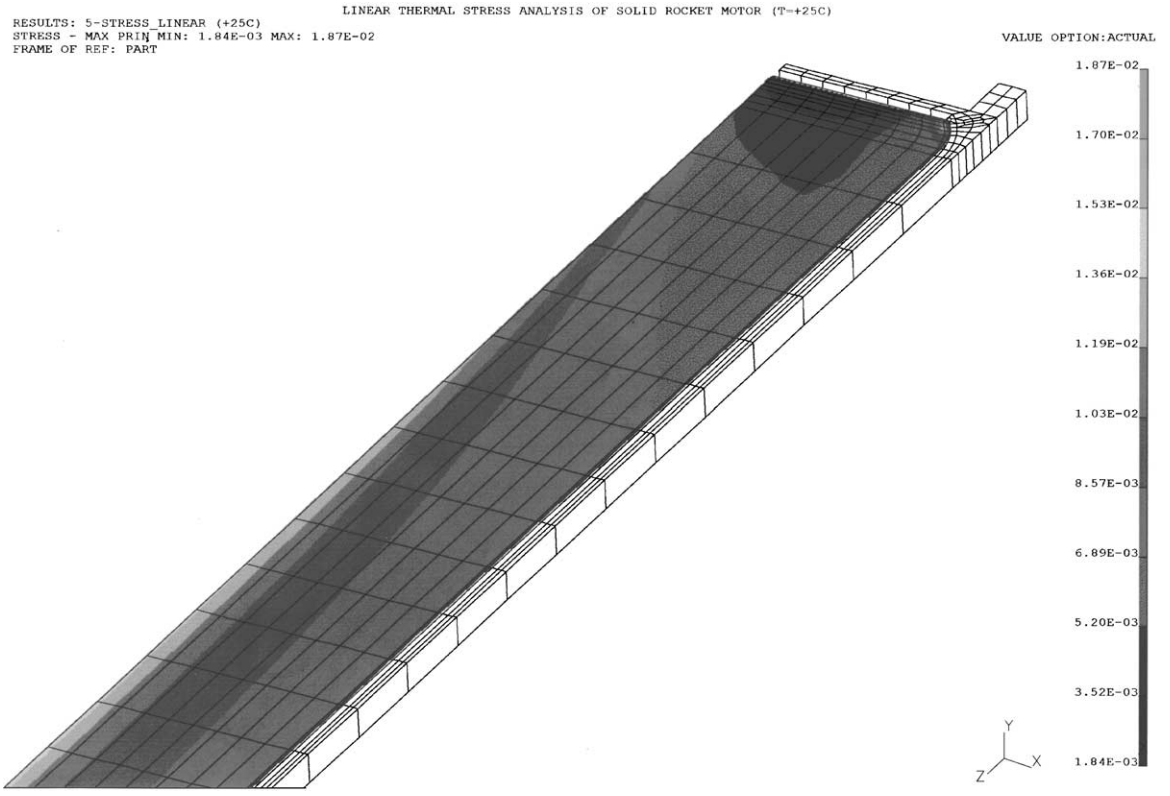

Fig. 7. The maximum principal stress distribution of HTPB propellant under thermal loading case 1 — quasi-elastic linear analysis.

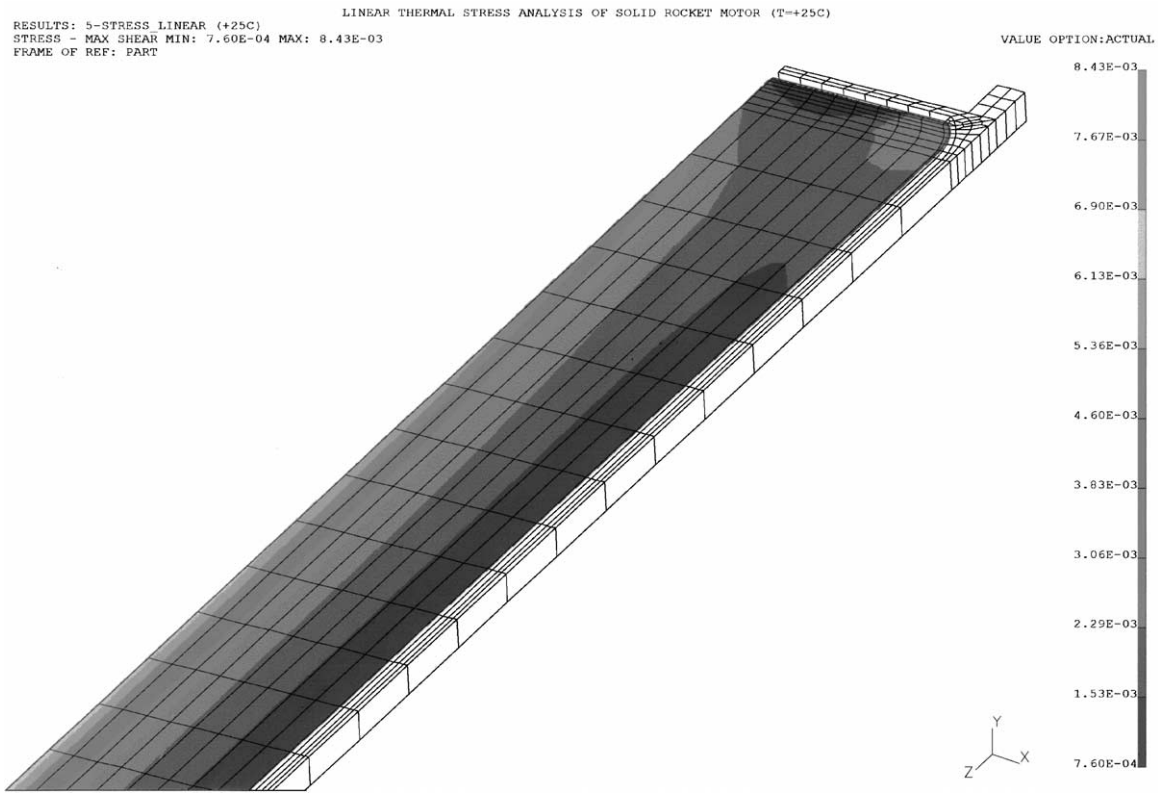

Fig. 8. The maximum shear stress distribution of HTPB propellant under thermal loading case 1 — quasi-elastic linear analysis.

4.1.2. Geometrical nonlinear thermoviscoelastic analysis

From the finite element simulation considering geometrical nonlinearity only, the maximum displacement is 1.03 mm, the maximum principal stress is 0.0187 kgf/mm^2, the maximum shear stress is 0.00844 kgf/mm^2, and the maximum principal strain is 4.98%.

4.1.3. Material nonlinear thermoviscoelastic analysis

From the finite element simulation considering material nonlinearity only, the maximum displacement is 1.02 mm, the maximum principal stress is 0.0189 kgf/mm^2, the maximum shear stress is 0.00845 kgf/mm^2, and the maximum principal strain is 4.97%.

4.1.4. Geometrical and material nonlinear thermoviscoelastic analysis

From the nonlinear finite element simulation considering the effects of large deformation and the variation of HTPB propellant bulk modulus with compressive stress, the maximum displacement is 1.02 mm, the maximum principal stress is 0.0189 kgf/mm^2, the maximum shear stress is 0.00845 kgf/mm^2, and the maximum principal strain is 4.97%. Because the stress response in this thermal loading case is tensile, the effect of nonlinear bulk modulus could be neglected and the

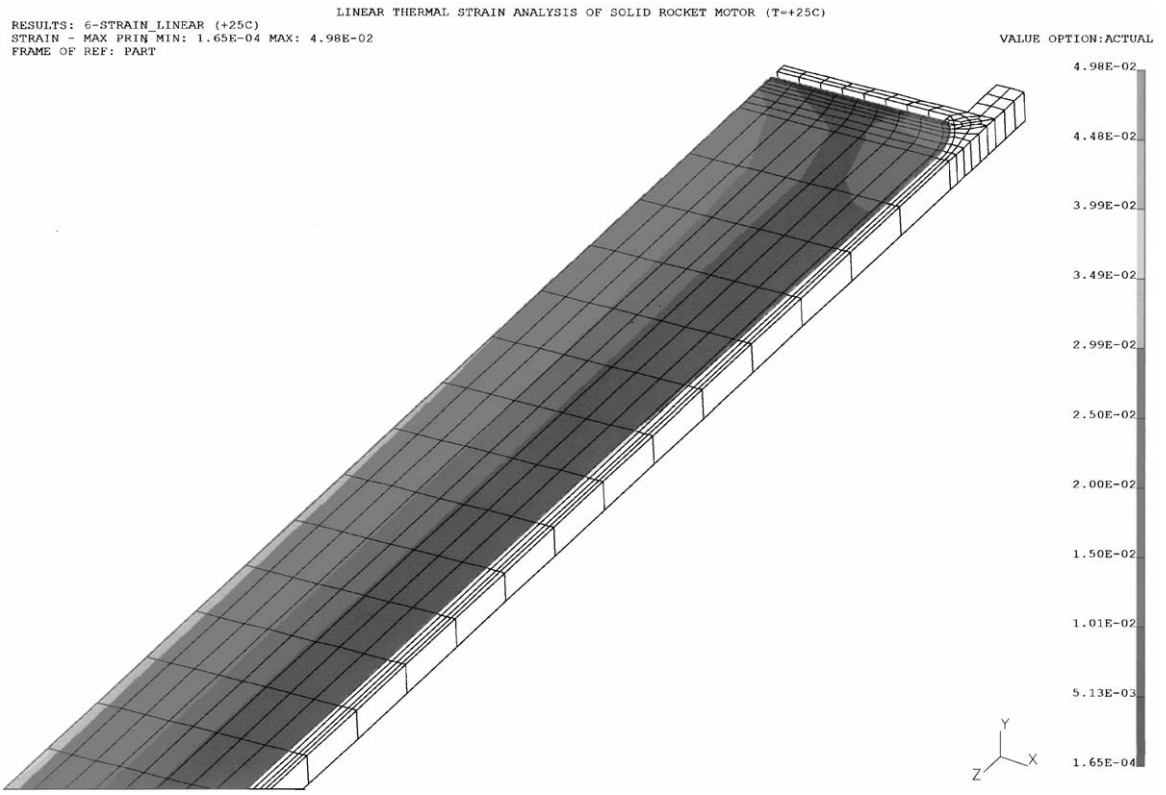

Fig. 9. The maximum principal strain distribution of HTPB propellant under thermal loading case 1 — quasi-elastic linear analysis.

difference between linear analysis and nonlinear thermoviscoelastic analysis is very small.

4.2. *Thermal loading case 2* ($T_{SF} = +160^{\circ}F, T_{operating} = +142^{\circ}F; t_{cooldown} = 5$days)

4.2.1. *Quasi-elastic linear analysis*

Under this thermal loading condition, the design load is defined as $T_{design} = (T_{operating} - T_{SF}) = -18^{\circ}F$ and the effective propellant modulus could be also obtained from Fig. 1, and the shift factor could also be obtained from Fig. 2. From the linear finite element simulation without the effect of geometrical and material nonlinearities to HTPB propellant, the maximum displacement is 0.223 mm, the maximum principal stress is 0.00407 kgf/mm^2, the maximum shear stress is 0.00185 kgf/mm^2, and the maximum principal strain is 1.079%.

4.2.2. *Geometrical nonlinear thermoviscoelastic analysis*

From the finite element simulation considering geometrical nonlinearity only, the maximum displacement is 0.223 mm, the maximum principal stress is 0.00407 kgf/mm^2, the maximum shear stress is 0.00185 kgf/mm^2, and the maximum principal strain is 1.079%.

4.2.3. Material nonlinear thermoviscoelastic analysis

From the finite element simulation considering material nonlinearity only, the maximum displacement is 0.223 mm, the maximum principal stress is 0.00405 kgf/mm^2, the maximum shear stress is 0.00186 kgf/mm^2, and the maximum principal strain is 1.08%.

4.2.4. Geometrical and material nonlinear thermoviscoelastic analysis

From the nonlinear finite element simulation considering the effects of large deformation and the variation of HTPB propellant bulk modulus with compressive stress, the maximum displacement is 0.223 mm, the maximum principal stress is 0.00405 kgf/mm^2, the maximum shear stress is 0.00186 kgf/mm^2, and the maximum principal strain is 1.08%. Because the stress response in this thermal loading case is tensile, the effect of nonlinear bulk modulus could be neglected and the difference between linear analysis and nonlinear thermoviscoelastic analysis is very small.

4.3. Thermal loading case 3 ($T_{SF} = +160^{\circ}F, T_{operating} = +169^{\circ}F; t_{cooldown} = 5$days)

4.3.1. Quasi-elastic linear analysis

Under this thermal loading condition, the design load is defined as $T_{design} = (T_{operating} - T_{SF}) = +9^{\circ}F$ and the effective propellant modulus could be also obtained from Fig. 1, and the shift factor could also be obtained from Fig. 2. From the linear finite element simulation without the effect of geometrical and material nonlinearities to HTPB propellant, the maximum displacement is -0.112 mm and the maximum shear stress is 0.000914 kgf/mm^2.

4.3.2. Geometrical nonlinear thermoviscoelastic analysis

From the finite element simulation considering geometrical nonlinearity only, the maximum displacement is -0.111 mm and the maximum shear stress is 0.000902 kgf/mm^2.

4.3.3. Material nonlinear thermoviscoelastic analysis

From the finite element simulation considering material nonlinearity only, the maximum displacement is -0.110 mm and the maximum shear stress is 0.00102 kgf/mm^2. Compare the nonlinear thermoviscoelastic analysis results between geometrical nonlinearity and material nonlinearity, one can see that the effect of material nonlinearity is more predominant as compared to the effect of geometrical nonlinearity.

4.3.4. Geometrical and material nonlinear thermoviscoelastic analysis

From the nonlinear finite element simulation considering the effects of large deformation and the variation of HTPB propellant bulk modulus with compressive stress, the maximum displacement is -0.110 mm and the maximum shear stress is 0.00102 kgf/mm^2 (see Fig. 10). This shows that there is a 11.597% increase in maximum shear stress as an outcome of the bulk modulus variation with compressive stresses.

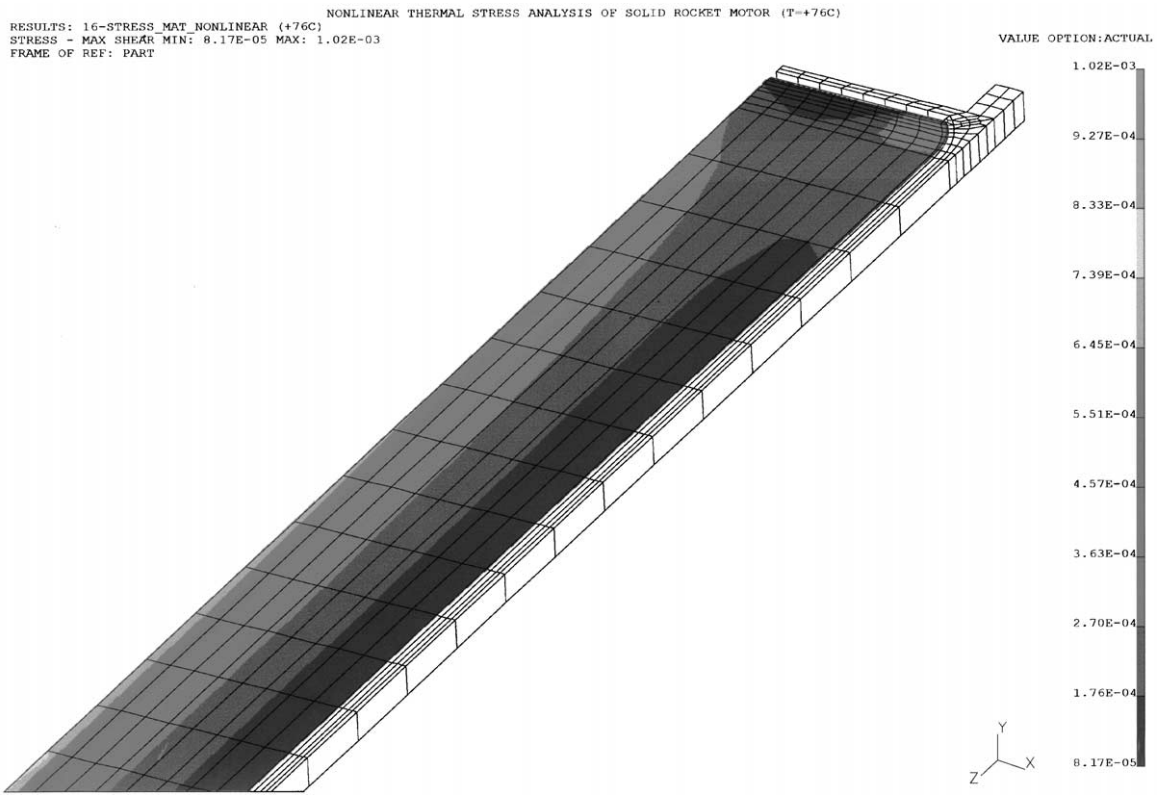

Fig. 10. The maximum shear stress distribution of HTPB propellant under thermal loading case 3 — nonlinear thermo-viscoelastic analysis.

4.4. Thermal loading case 4 ($T_{SF} = +160^{\circ}F, T_{operating} = +178^{\circ}F; t_{cooldown} = 5days$)

4.4.1. Quasi-elastic linear analysis

Under this thermal loading condition, the design load is defined as $T_{design} = (T_{operating} - T_{SF}) = +18^{\circ}F$ and the effective propellant modulus could also be obtained from Fig. 1, and the shift factor could also be obtained from Fig. 2. From the linear finite element simulation without the effect of geometrical and material nonlinearities to HTPB propellant, the maximum displacement is -0.223 mm and the maximum shear stress is $0.001833\ kgf/mm^2$.

4.4.2. Geometrical nonlinear thermoviscoelastic analysis

From the finite element simulation considering geometrical nonlinearity only, the maximum displacement is -0.220 mm and the maximum shear stress is $0.001809\ kgf/mm^2$.

4.4.3. Material nonlinear thermoviscoelastic analysis

From the finite element simulation considering material nonlinearity only, the maximum displacement is -0.218 mm and the maximum shear stress is $0.00225\ kgf/mm^2$. Compare the nonlinear

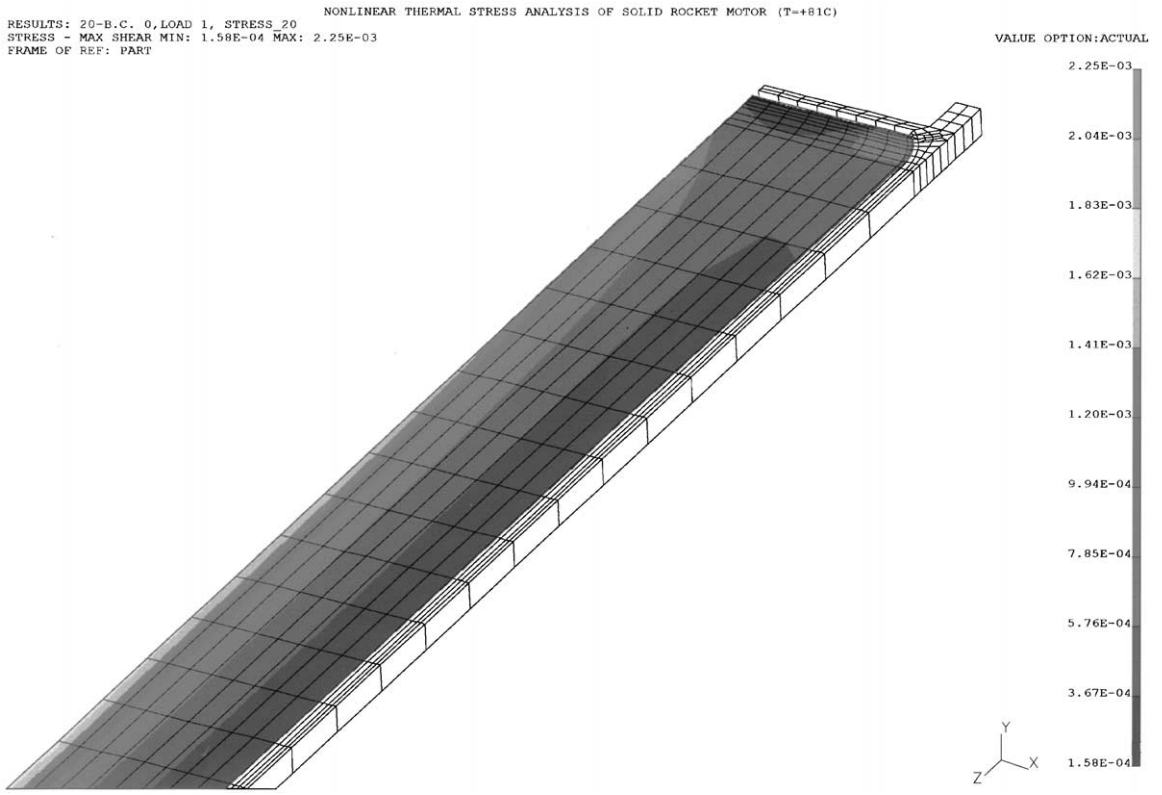

Fig. 11. The maximum shear stress distribution of HTPB propellant under thermal loading case 4 — nonlinear thermo-viscoelastic analysis.

thermoviscoelastic analysis results between geometrical nonlinearity and material nonlinearity, one can see that the effect of material nonlinearity is more predominant as compared to the effect of geometrical nonlinearity.

4.4.4. Geometrical and material nonlinear thermoviscoelastic analysis

From the nonlinear finite element simulation considering the effects of large deformation and the variation of HTPB propellant bulk modulus with compressive stress, the maximum displacement is -0.218 mm and the maximum shear stress is $0.00225\ \mathrm{kgf/mm^2}$ (see Fig. 11). This shows that there is a 22.75% increase in maximum shear stress as an outcome of the bulk modulus variation with compressive stresses.

4.5. Thermal loading case 5 ($T_{SF} = +160^{\circ}\mathrm{F}, T_{operating} = +205^{\circ}\mathrm{F}; t_{cooldown} = 5\mathrm{days}$)

4.5.1. Quasi-elastic linear analysis

Under this thermal loading condition, the design load is defined as $T_{design} = (T_{operating} - T_{SF}) = +45^{\circ}\mathrm{F}$ and the effective propellant modulus could also be obtained from Fig. 1, and the shift factor could also

be obtained from Fig. 2. From the linear finite element simulation without the effect of geometrical and material nonlinearities to HTPB propellant, the maximum displacement is -0.558 mm and the maximum shear stress is 0.00458 kgf/mm^2.

4.5.2. Geometrical nonlinear thermoviscoelastic analysis

From the finite element simulation considering geometrical nonlinearity only, the maximum displacement is -0.551 mm and the maximum shear stress is 0.00452 kgf/mm^2.

4.5.3. Material nonlinear thermoviscoelastic analysis

From the finite element simulation considering material nonlinearity only, the maximum displacement is -0.546 mm and the maximum shear stress is 0.00597 kgf/mm^2. Compare the nonlinear thermoviscoelastic analysis results between geometrical nonlinearity and material nonlinearity, one can see that the effect of material nonlinearity is more predominant as compared to the effect of geometrical nonlinearity.

4.5.4. Geometrical and material nonlinear thermoviscoelastic analysis

From the nonlinear finite element simulation considering the effects of large deformation and the variation of HTPB propellant bulk modulus with compressive stress, the maximum displacement is -0.546 mm and the maximum shear stress is 0.00597 kgf/mm^2 (see Fig. 12). This shows that there is a 30.316% increase in maximum shear stress as an outcome of the bulk modulus variation with compressive stresses.

5. Results and discussion

1. Results show that the material nonlinear effect is important for structural integrity of solid propellant grains under higher temperature surrounding, and this effect is not obvious under lower temperature surrounding. Under a lower temperature surrounding, the thermal stress response of solid rocket motor is tensile, bulk modulus could be considered as invariant, and linear analysis could be adopted. But for higher temperature surrounding, the thermal stress response of solid rocket motor may be compressive, the effect of bulk modulus variation with compressive stress should be considered, and nonlinear analysis should be used. From the results of maximum shear stress increase analyzed by thermal loading case 1 (0.0%), thermal loading case 2 (0.0%), thermal loading case 3 (11.597%), thermal loading history assumption 4 (22.75%) and thermal loading case 5 (30.316%), diverse thermal loading cases could obtain different results (see Fig. 13). In addition, Fig. 13 shows that the differences between linear and nonlinear analysis results become more and more predominant as temperature increases.
2. Numerical results presented in this article show that the maximum shear stress obtained from the nonlinear analysis considering bulk modulus variation with compressive stress are remarkably higher than those obtained from the linear analysis assuming a constant bulk modulus. In addition, the effect of material nonlinearity is more predominant as compared to the effect of geometrical nonlinearity.

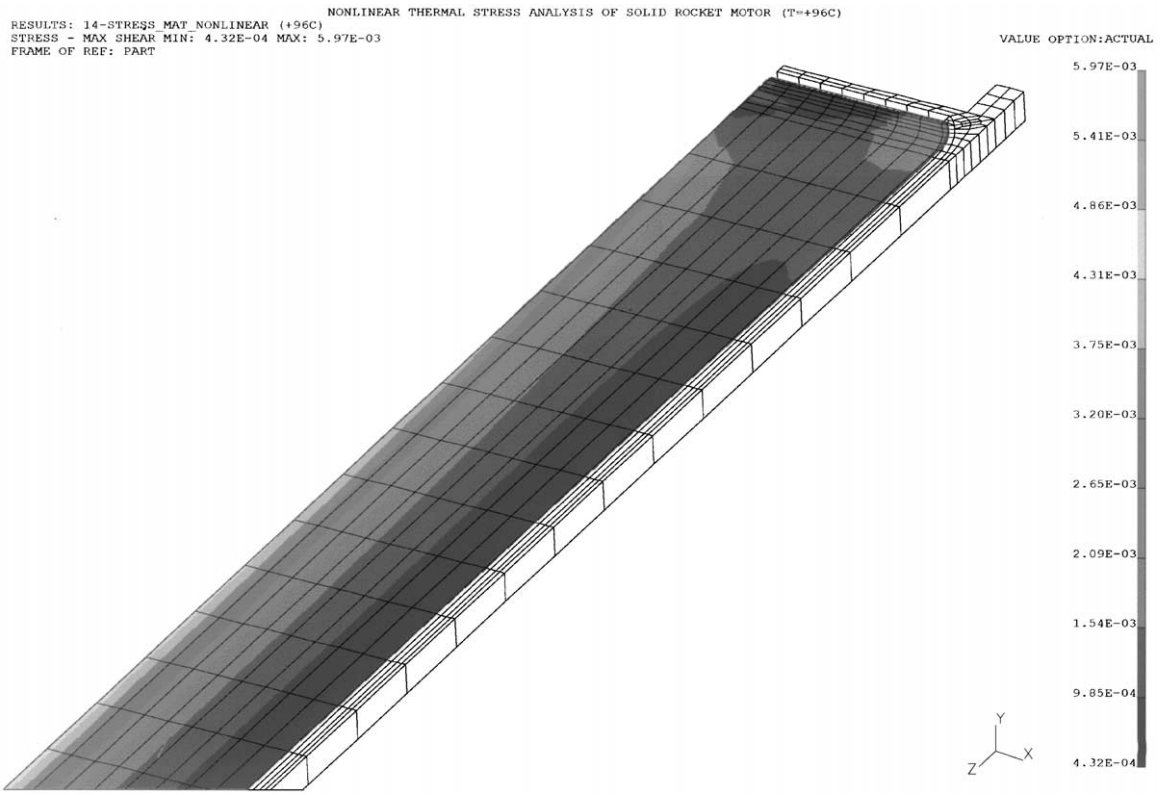

Fig. 12. The maximum shear stress distribution of HTPB propellant under thermal loading case 5 — nonlinear thermo-viscoelastic analysis.

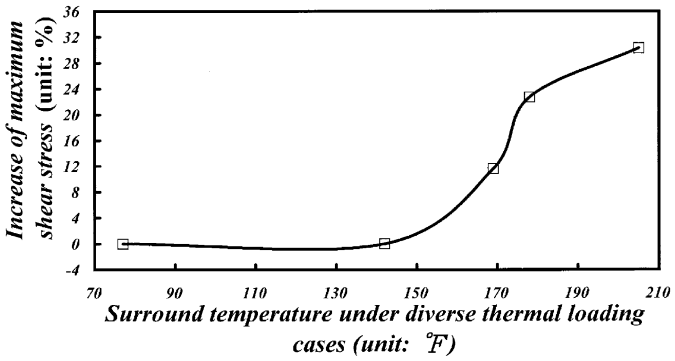

Fig. 13. The increase in maximum shear stress for HTPB propellant under diverse thermal loading cases.

3. Comparing the nonlinear analysis results under temperature loading presented in this article with those for pressure load from [14], some interesting difference because of different loading type could be found. In pressure loading case [14], the displacements and strains obtained from the nonlinear analysis are considerably lower than those obtained from the linear analysis with initial

bulk modulus value. But for thermal loading case presented in this article, there is an increase in maximum shear stress as an outcome of the bulk modulus variation with compressive stresses.

4. Because the configuration of solid rocket motor is too complex to predict the critical area and failure mode in the design phase using a simple analytical model, the finite element simulation becomes the best method to obtain the stress distribution under diverse loading cases. Without the numerical analysis, designers need much more time to try and error to get a feasible design type accompanied by many experimental data. Therefore, the finite element analysis can reduce project span time and save the total project cost.

6. Conclusions

An elaborate and extensive structural analysis of solid propellant grains considering the geometrical and material nonlinear effect under thermal loading case was carried out using a commercial analysis FEA software package [23,24] with a CAE pre–post processor [25]. A 3-D solid model was adopted to obtain detailed analysis results. In order to simulate the material and geometrical nonlinearities, a step-by-step finite element model accompanied by concepts of time–temperature shift principle, reduced integration and thermorheologically simple material assumption was used. Results show that the material nonlinear effect is important for structural integrity of solid propellant grains under higher temperature surrounding, the effect of nonlinearity is not obvious under lower temperature surrounding, and the differences between linear and nonlinear analysis results become more and more predominant as temperature increases. In addition, the maximum shear stress obtained from the nonlinear simulation considering bulk modulus variation with compressive stresses are higher than those from linear simulation, and the effect of material nonlinearity is more predominant as compared to the effect of geometrical nonlinearity. From the work of linear and nonlinear analyses, the nonlinear thermoviscoelastic analysis highlighted several areas of interest and a more accurate and reasonable result could be obtained for an engineer.

References

[1] O.C. Zienkiewicz, K. Morgan, Finite Elements and Approximation, Pineridge, Swansea, 1983.
[2] K.J. Bathe, Finite Element Procedures in Engineering Analysis, Prentice-Hall, Englewood Cliffs, NJ, 1982.
[3] G.J. Svob, K.W. Bills Jr., Predictive surveillance technique for air-launched rocket motors, J. Spacecr. 21 (2) (1984) 162–167.
[4] K.W. Bills Jr., Structural design nomograph for thermal cycling of tactical rocket propellants, NWC Tech. Memo 3365, December 1977.
[5] Shiang-Woei Chyuan, Life assessment of solid-propellant structure under thermal cycling (structure over test) using structural design nomograph, Proceedings of The Fifth ROC Symposium on Fracture Science, 1998, pp. 31–38 (in Chinese).
[6] A.G. Christiansen, L.H. Layton, R.L. Carpenter, HTPB propellant aging, J. Spacecr. 18 (3) (1981) 211–215.
[7] W.M. Chang, S.W. Chyuan, N.C. Shieh, Aging life prediction of polymer material structure using MSC/NASTRAN and Layton equation, MSC Taiwan Users' Conference Proceedings, 1994 (in Chinese).
[8] Shiang-Woei Chyuan, Finite element simulation on solid-propellant structure under thermal shock loads, Proceedings of The 14th National Conference on Mechanical Engineering, The Chinese Society of Mechanical Engineers, Chung-Li, Taoyuan, Taiwan, R.O.C., December 1997, pp. 100–107 (in Chinese).

[9] Shiang-Woei Chyuan, Modeling of transient thermal mechanical response using finite element method (MSC/NASTRAN), MSC Taiwan Users' Conference Proceedings, 1993 (in Chinese).
[10] J.T. Chen, S.-Y. Leu, Finite element analysis, design and experiment on solid propellant motors with a stress reliever, Finite Elements Anal. Des. 29 (1998) 75–86.
[11] Solid Propellant Grain Structural Integrity Analysis, NASA SP 8073, 1973.
[12] S.L. Lin, I.C. Tsai, N.C. Shieh, MSC/NASTRAN stress analysis application in linear viscoelastic material problem, MSC Taiwan Users' Conference Proceedings, 1989 (in Chinese).
[13] Shiang-Woei Chyuan, A study of loading history effect for thermoviscoelastic solid propellant grains, Comput. Struct. 77 (2000) 735–745.
[14] M.K. Jana, K. Renganathan, G. Venkateswara Rao, Effect of bulk modulus variation with pressure in propellant grain elastic stress analysis, Comput. Struct. 26 (5) (1987) 761–766.
[15] C.A. Brebbia, J.C.F. Telles, L.C. Wrobel, Boundary Element Techniques, Springer, Berlin, Heidelberg, 1984.
[16] J.T. Chen, H.-K. Hong, S.W. Chyuan, Boundary element analysis and design in seepage problems using dual integral formulation, Finite Elements Anal. Des. 17 (1994) 1–20.
[17] Shiang-Woei Chyuan, Finite element simulation of a twin-cam 16-valve cylinder structure, Finite Elements Anal. Des. 35 (2000) 199–212.
[18] S.W. Chyuan, C.Y. Chiou, Application and modeling of finite element method on structural mechanics and thermal analysis, ABSTRACTS of Invited Lectures and Short Communications Delivered at the Sixth International Colloquium on Numerical Analysis and Computer Science with Applications, August 13–17, 1997, Plovdiv, Bulgaria, pp. 31–33.
[19] M.L. William, Structural analysis of viscoelastic materials, AIAA J. 5 (1964) 785–808.
[20] W.N. Findley, J.S. Lai, K. Onoran, Creep and Relaxation of Nonlinear Viscoelastic Materials, North-Holland, Amsterdam, 1976.
[21] L.W. Morland, E.H. Lee, Stress analysis of linear viscoelastic materials with temperature variation, Trans. Soc. Rheol. 4 (1960) 233–263.
[22] JANNAF Solid Propellant Structural Integrity Handbook, Minimum standard structural analysis procedures for solid rocket grains under thermal and pressurization loading, CPIA Publication No. 230, Chemical Propulsion Agency, The Johns Hopkins University, Applied Physics Laboratory, Laurel MD, February 1987.
[23] Sang, H. Lee, MSC/NASTRAN Nonlinear Analysis Handbook (Version 67), The MacNeal-Schwendler Corporation, 815 Colorado Boulevard, Los Angeles CA 90041-1777, 1992.
[24] J.T. Chen, S.L. Lin, C.Y. Chiou, S.W. Chyuan, J.Y. Hwang, W.R. Harn, W.T. Chin, Finite Element Analysis and Engineering Applications Using MSC/NASTRAN, Northern Gate Publication, Taipei, Taiwan, 1996 (in Chinese).
[25] I-DEAS User's Guide, Finite Element Modeling, SDRC, 1990.